

# Low-cost iron-on grids applied to plastic strain analysis

Tito Marin<sup>1</sup> – Gianni Nicoletto<sup>2</sup>

## Abstract

Geometric moiré is suitable for relatively large strain analysis due to its limited sensitivity. In this paper a procedure of grating preparation using affordable iron-on paper is applied to the plastic strain analysis of thin specimens made of low carbon steel. A companion elastic-plastic finite element analysis is carried out to provide reference data. The aim is to assess the range of practical applicability of the technique and to highlight the limits.

## Összefoglalás

**Olcsó, öntapadós rács alkalmazása a képlékeny alakváltozás elemzéséhez.** A moiré ábra, korlátozott érzékenységgel, megfelelő a viszonylag nagy alakváltozás elemzéséhez. A cikk ismerteti a sima és a közepén átfúrt lapos, kis széntartalmú acél próbatestek képlékeny alakváltozása elemzésének öntapadós ráccsal húzó kísérlettel, illetve a rugalmas-képlékeny végeelem-módszerrel számítással meghatározott eredményeit. Az összehasonlítás célja: megállapítani az öntapadós rács gyakorlati alkalmazhatóságának tartományát és korlátját.

## Introduction

Optical methods have become fairly widespread tools in experimental strain analysis and are specifically useful when a full-field capability is required, [1]. Geometric moiré is one of the earliest optical methods and is based on the superposition of a reference grating and a specimen grating. For its theoretical simplicity and ease of application it is useful as an experimental support of the teaching of strength of materials, [2]. Due to its inherently limited sensitivity (i.e.  $f = 40$  lines/mm) it is suited only for relatively large strain analysis, so that typical applications concern polymeric materials, like plastics and rubber, or metals strained into the plastic range.

In all the moiré methods the quality of the gratings is critical because it affects the visibility of moiré fringes, moreover the grating frequency,  $f$ , dictates the displacement sensitivity ( $1/f$ ). Gratings are regular arrays of lines that can be produced in different ways; as a general rule the higher the frequency the higher the cost. In this paper an inexpensive grating preparation procedure is adopted and, combined with the geometric moiré method, is applied in strain analysis of thin specimens made of mild steel. A first tensile test of a smooth specimen is conducted in order to establish the suited range of strain and to calibrate the procedure, then the technique is applied to the more challenging plastic strain analysis of a notched specimen.

The aim of the work is to test and improve on the grating preparation procedure in order to maximize fringe visibility and contrast, and also to determine the applicability range and the limits of the technique.

## Methodology

### Basic of geometric moiré

In the geometric moiré method, a grating is firmly applied to the specimen so that it deforms in accordance with the specimen surface.

Department of Industrial Engineering, University of Parma  
Parco Area delle Scienze 181/A, 43100 Parma, Italy

<sup>1</sup> marin@me.unipr.it <sup>2</sup> nick@me.unipr.it

Superposition of a reference (non-deformed) grating to the specimen grating results in fringe patterns associated to the in-plane displacement components  $U_j(x,y)$ . They are determined according to the following equations

$$U_i = g N_i = N_i / f \quad i,j=x,y \quad (1)$$

in which  $f$  and  $g$  are the reference grating frequency and pitch and  $N_j$  is the fringe order in the  $x$  and  $y$  directions, respectively. Strains are the spatial derivatives of the in-plane displacements. Therefore, the following simple relationships between grating and fringe pattern characteristics (moiré fringe spacing  $G_j$  and fringe frequency  $F_j$ ) are used:

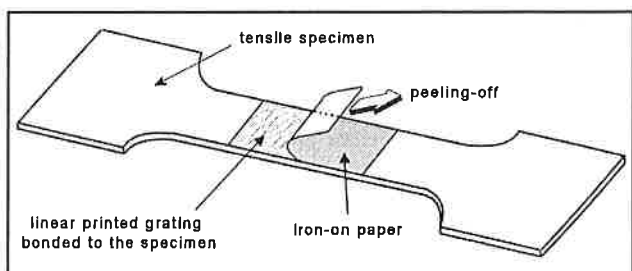
$$\varepsilon_{ij} = U_{i,j} = 1/2(g_i/G_j + g_j/G_i) = 1/2(F_j/f_i + F_i/f_j) \quad i,j=x,y \quad (2)$$

### Grating preparation

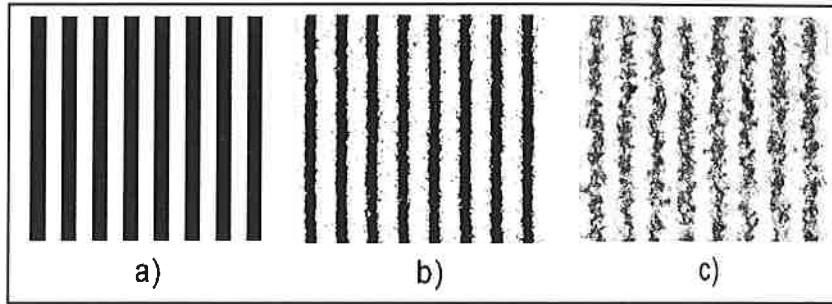
The linear gratings used for these experiments were generated with a simple computer routine that allows to set the spacing between adjoining lines, [3]. The reference gratings were printed on ordinary overhead transparencies with a 600 dpi HP laser printer, while the specimen gratings were printed on Epson iron-on cool-peel transfer paper with a 600 dpi HP inkjet printer. The iron-on paper is a particular paper typically used for customizing T-shirts by transferring printed images. It consists of three different stacked layers, the bottom layer is paper serving as backing material, the top layer absorbs ink and is transferred to the specimen, [4]. The middle layer is a thin polymeric film that prevents ink permeating to the bottom paper layer, it also separates top and bottom layers when peeling off the paper backing after the printed layer is transferred to the specimen.

The ironing is obviously not necessary, actually the transfer of the grating onto the specimen surface consists of the following steps:

1. A 3M spray adhesive is employed to bond the grating and the specimen together. This operation must be carefully performed to align grating lines and specimen major axes. Twisting or wrapping of the printed paper must be avoided not to induce any initial fictitious deformations.
2. Moderate uniform pressure is applied to squeeze out the adhesive in excess and to minimize grating thickness.
3. After the curing time, the outer layers of the iron-on paper are then gently peeled off while leaving only the printed grating on the specimen surface, see Figure 1. The average thickness of the resulting coating made of the printed layer and the adhesive layer is approx. 80  $\mu\text{m}$ .



1. ábra. Az öntapadós rács felvitele a próbatest felületére  
Fig. 1 – Procedure adopted to transfer the grating onto the specimen surface



2. ábra. A rácskontraszt ideális (a), a próbatest felületén megjelenő (b), illetve referencia (c) változata; rácsosztás: 169  $\mu\text{m}$

Fig. 2 – a) Ideal grating, b) specimen grating, c) reference grating. Pitch=169  $\mu\text{m}$

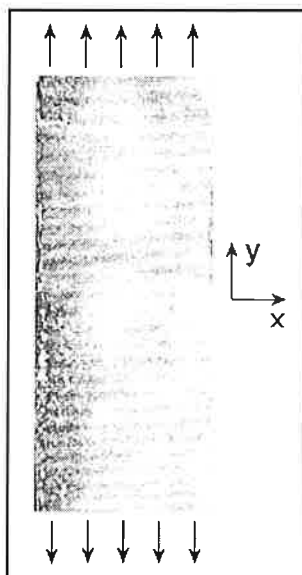
Since the higher the grating frequency  $f$  the higher the sensitivity, an effort is made to obtain high frequency gratings of good quality. Some spreading of ink is unavoidable but overlapping of lines is not acceptable, therefore, due to the resolution of the printers employed (600 dpi), the best compromise was reached by printing each line separated by three non-printed lines, [5]. This results in a grating frequency  $f=5.9$  line/mm. Accordingly, the contour interval (displacement per fringe order) is  $f^{-1}=169 \mu\text{m}$ .

The use of a white adhesive is recommended to enhance the fringe contrast. It is worth noting that the laser printer could not be used for the iron-on paper because, during the printing process, the paper gets warmer and melts.

Figure 2 shows an ideal high contrast grating compared with the printed gratings. The reference grating presents an optimum contrast and the lines are perfectly spaced equally and straight. In the specimen grating instead, the effects of roughness and porosity of the paper are evident so that the optical contrast is quite affected, nevertheless the lines are, in average, still straight.

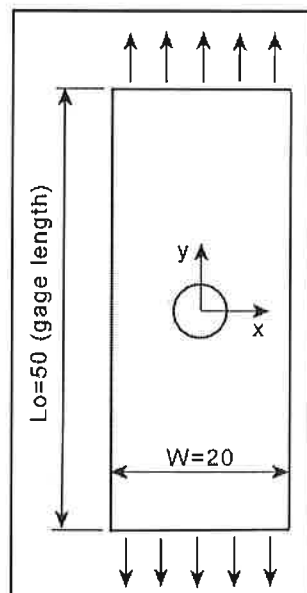
### Calibration

A preliminary tensile test was performed in a MTS servo-hydraulic loading machine on a smooth specimen. The specimen (thickness=0.65mm, width  $W=20\text{mm}$ , gage length  $L_0=50\text{mm}$ ) was machined from a cold rolled sheet of low carbon steel (DC01-UNI EN 10130,



3. ábra. Sima próbatesten a rácsközök megnyúlása az  $\epsilon_y = 11\%$  névleges értékénél

Fig. 3 – Smooth specimen: fringe pattern at nominal strain  $\epsilon_y=11\%$



4. ábra. A bemetszett próbatest méretei

Fig. 4 – Notched specimen geometry

$\sigma_{p0.2}=228\text{MPa}$ ,  $\sigma_R=297\text{MPa}$ ,  $A\%=23,5\%$ ). On the specimen a grating with lines parallel to the  $x$ -direction was prepared to obtain the in-plane displacement component  $U_y$  and the longitudinal strain  $\epsilon_y$  in the loading direction,  $y$ . The captured images of the moiré fringes were subsequently elaborated by means of a digital imaging software to reduce noise and improve the contrast. This step is crucial, particularly when fringes are faint. A typical fringe pattern of the tensile test is shown in Figure 3: fringes are parallel and perpendicular to the horizontal load direction, as expected from a theoretical point of view. Moiré fringes were continuously recorded, through a CCD, during the tensile test up to specimen rupture to determine the range of applicability of the technique. They were not distinguishable below a deformation of approx. 2% while the upper limit in strain was about 17%. From then onward the fringes became less clear. This is due to damage of the specimen grating.

After the basic calibration, the technique was applied to a notched specimen, Figure 4, where a not uniform state of strain and strong gradients are expected. A parallel finite element analysis of the experiment was also carried out in order to provide reference data for the assessment of the accuracy.

### Application

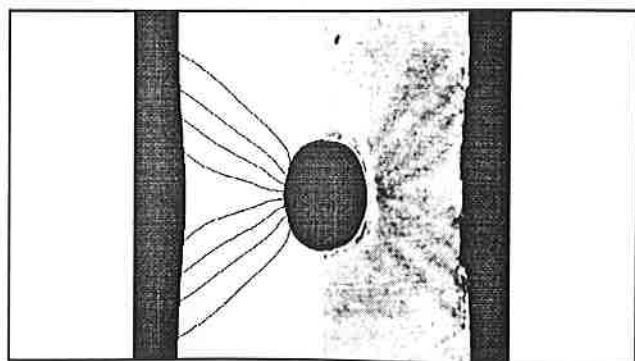
After the basic calibration, the technique was applied to a notched specimen, Figure 4, where a not uniform state of strain and strong gradients are expected. A parallel finite element analysis of the experiment was also carried out in order to provide reference data for the assessment of the accuracy.

### Experimental details

The notched specimen had the identical geometry of the smooth one but with a circular 6-mm diameter hole in the centre and it was machined from the same metal sheet. The grating lines were parallel to the  $x$ -direction to obtain the displacement component  $U_y$  and the strain component  $\epsilon_y$ . The experimental procedure is the same described before.

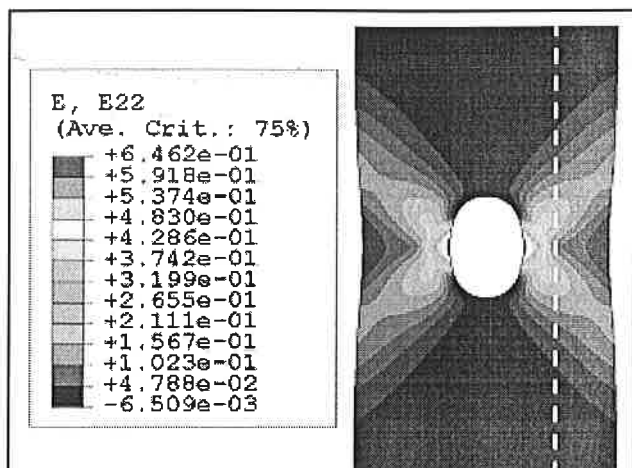
### Finite element analysis

A non-linear elastic-plastic finite element simulation of the tensile experiment on the notched specimen was developed using the ABAQUS code, [6], to compare the results with the experimental ones. A two-dimensional model was created using quadratic 8-node plane stress elements and the constitutive stress-strain law of the tensile test was introduced point-by-point to accurately describe the material behaviour. The displacement given by an extensometer during the experiment (gage length  $L_0=50\text{mm}$ ) was adopted as boundary condition in the simulation.



5. ábra. Az  $U_y = \Delta L/L_0 = 1,75 \text{ mm}$  értékhez tartozó, végelem-módszerrel (FEM) számított (balra), illetve mért (jobbra) rácsvonal-rajzolat összehasonlítása

Fig. 5 – FEM fringes (on the left) vs. experimental (on the right) when  $U_y=\Delta L/L_0=1.75 \text{ mm}$



6. ábra. A nyúlás végeselem-módszerrel (FEM) számított  $\epsilon_y$  összetevője

Fig. 6 – FEM strain component  $\epsilon_y$

### Results and discussion

Figure 5 shows the comparison between the numerical moiré fringes with the actual image of the specimen and the experimental moiré fringes. They are found to match in a satisfactory way. The fringes loose definition in the immediate vicinity of the hole where the numerical fringes show a strong strain gradient. The severity of the gradient is also visible in the strain  $\epsilon_y$  map shown in Figure 6. Application of the Von Mises plasticity criterion would show plastic flow zones spreading out of the central hole in the  $\sim 45^\circ$  directions.

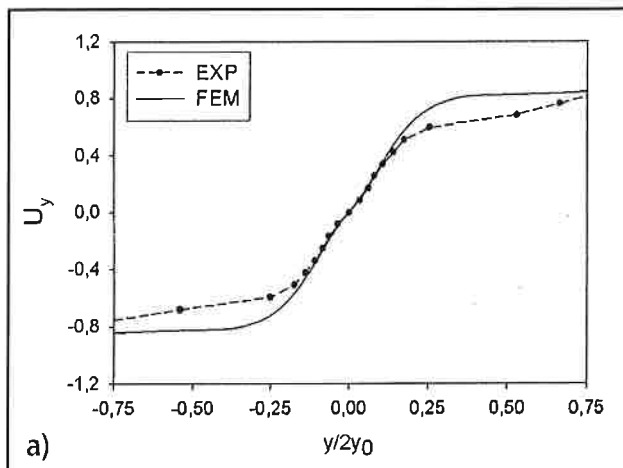
Assessment of the experiment was carried out in detail along some vertical lines. The results presented here concern the dotted line of Figure 6. The comparison between the experimental in-plane displacement component and the FE counterpart is quite good especially in the central high strained region while some deviations are observed at a distance from the mid plane, where the level of plastic strain is relatively limited, Figure 7. From the computational point of view this condition of initial plasticity is the most sensitive to the constitutive law.

Computed strains along the same line is mapped in Figure 7 b) to provide direct comparison with the experiments. The local finite difference definition of strain was used to obtain strain estimate from neighbouring fringes. The strain  $\epsilon_y$  is averaged between adjacent fringes and, despite of the shortage of them, can be extracted with reasonable accuracy. The continuous and regular variation in FE result is confirmed by the moiré-based results. The two strain peaks symmetrically located with respect to the centre line as well as the strong strain gradient are determined from the moiré fringes. The difference between experiment and analysis is found in the area where the material deforms elastically and the moiré sensitivity is not adequate.

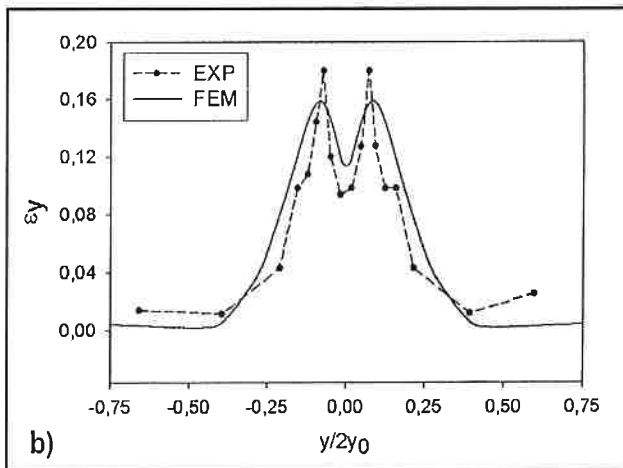
### Conclusions

In this work geometric moiré and the iron-on grating preparation procedure were applied to plastic strain analysis of steel specimens, smooth and notched. One of the objectives of this study was to test and improve on the simple and inexpensive grating preparation procedure in order to maximize fringe visibility and contrast. It can be stated that moiré fringes are in general quite clear and stable although the sensitivity is inherently limited.

A second objective was to determine the applicability range of the moiré method. In spite of the not sophisticated tools used, the accuracy is quite satisfying. Based on the direct comparison to a companion elastic-plastic finite element analysis of the notch test it is confirmed that the resolution is appropriate for large deformations, i.e. plastic strain, and



a)



b)

7. ábra. A 6. ábrán szaggatott vonallal jelölt helyek számított (FEM) és mért értékeinek összehasonlítása: a) a síkírányú elmozdulás  $U_y$  összetevője, b) a közvetlen nyúlás  $\epsilon_y$  összetevője

Fig. 7 – Comparison of experimental and FEM results along the dotted line of Figure 6.

a) in-plane displacement component  $U_y$ , b) direct strain  $\epsilon_y$

that the upper limit (about 17%) is dictated by the incipient damage of the grating.

### Bibliography

- [1] A.-S. Kobayashi ed.: Handbook on Experimental Mechanics, Prentice-Hall, 1987
- [2] G. T. Reid: Moiré fringes in metrology, *Opt. Laser Eng*, 5 (2), 1984, pp. 63-93
- [3] <http://www.me.washington.edu/faculty/tuttle.html>
- [4] N.-S. Liou, C.-Y. Huang: Fourier transform moiré strain analysis by using cross gratings produced from iron-on paper and inkjet printer, *Polym. Test.*, Vol. 22, 2003, pp.487-490
- [5] M. E. Tuttle: Demonstrating moiré fringes using gratings produced with a laser printer, *Experimental Techniques*, Vol. 21, 1997, pp.19-22
- [6] ABAQUS, version 6.4, Hibbitt, Karlsson and Sorensen, Inc. Pawtucket, RI, 2002
- [7] P. Livieri, G. Nicoletto: Elasto-plastic strain concentration factors in finite thickness plates, *Journal of Strain Analysis*, Vol. 37, N. 5, 2002, pp. 1-6
- [8] T. Marin, G. Nicoletto: Determination of elastic-plastic strains using affordable iron-on grids, Proceedings of ICEM12 International conference on experimental mechanics, Bari, Italy, 2004